

Quantum coherence in ion channels: Resonances, Transport and Verification

Alipasha Vaziri

Janelia Farm Research Campus, Howard Hughes Medical Institute 19700 Helix Drive Ashburn, VA 20147, USA

Martin B. Plenio

Institut für Theoretische Physik, Albert-Einstein Allee 11, Universität Ulm, Germany

Recently it was demonstrated that long-lived quantum coherence exists during excitation energy transport in photosynthesis. It is a valid question up to which length, time and mass scales quantum coherence may extend, how to one may detect this coherence and what if any role it plays for the dynamics of the system. Here we suggest that the selectivity filter of ion channels may exhibit quantum coherence which might be relevant for the process of ion selectivity and conduction. We show that quantum resonances could provide an alternative approach to ultrafast 2D spectroscopy to probe these quantum coherences. We demonstrate that the emergence of resonances in the conduction of ion channels that are modulated periodically by time dependent external electric fields can serve as signatures of quantum coherence in such a system. Assessments of experimental feasibility and specific paths towards the experimental realization of such experiments are presented. We show that this may be probed by direct 2-D spectroscopy or through the emergence of resonances in the conduction of ion channels that are modulated periodically by time dependent external electric fields.

PACS numbers:

A wide variety of transport processes on all length and time-scales are of fundamental importance for the function of biological systems. For a long time it was assumed that these transport processes may be modelled accurately as classical random processes and the possible relevance of non-classical phenomena such as quantum coherence was mostly ignored. The experimental demonstration of the presence of long-lived quantum coherence in the photosynthetic energy transfer at cryogenic temperatures [1, 2] and room temperature [3] has forced a critical reevaluation of this position. As a consequence, the detailed experimental and theoretical study of quantum coherence in bio-molecular systems and its possible relevance to explain functional properties of those systems is currently receiving rapidly increasing attention.

The transport in the photosynthetic complex or the reactions during the first steps in vision [4, 5] involve initiation and fast transfer of electronic excitation via an absorbed photon on the femtosecond time scale. Given that these systems have been evolutionary optimized to function at highest efficiencies (e.g. human vision has few photon sensitivity [6, 7]), they might seem to naturally suggest themselves as areas to look for quantum coherence. More generally however, on time scales that are short compared to the decoherence time of an observed biological process quantum mechanical coherence can be expected to occur and play a role in biological function despite (or even because of) the strong interaction of bio-molecular systems with their environment.

Indeed, there may be non-trivial effects, positive or negative, due to the interplay between quantum coherent dynamics and decoherence from environments. In models of photosynthetic energy transfer it has been shown that compared to the purely quantum coherent case the efficiency of excitation transfer is enhanced by the presence

of dephasing noise [8, 9] originating from an environment of vibrational modes. It was shown that the transport performance of the system is optimal when it is neither fully decohered and hence classical nor fully quantum coherent. The mechanisms underlying this phenomenon have been identified and understood to apply more generally beyond the specific setting of energy transport in photosynthetic complexes [10, 11] and optimized transport settings in simpler structures have been determined [12]. The role of quantum coherence in other light harvesting systems [13] and for speed-up at early stages of the transport process has been examined [14] and the presence of entanglement [10, 15] has been studied in some detail.

These results provide further motivation to explore the relevance of quantum coherence and decoherence for transport in other biological entities. Here we discuss another system in which the interplay between quantum coherence and environmental noise could be responsible to explain some of the functional observations of the system.

Ion-channels are protein complexes that regulate the flow of particular ions across the cell membrane and are essential for a large range of cellular functions [16]. Besides their role in neuronal communications in which voltage gated channels and ligand gated channels are involved in the generation of action potentials and mediating synaptic release, more generally ion-channels play a key role in processes that rely on fast responses on the bio-molecular scale. Examples include muscle contraction, epithelial transport and T-cell activation [16, 17]. Structurally, ion-channels are integral transmembrane protein complexes with multiple subunits whose relative spatial arrangement forms a pore through which ions can flow in or out of the cell along a concentration gradient. A

common feature in a large number of ion-channels is the presence of a gate that can be activated by chemicals, voltage, light or mechanical stress and a selectivity filter which is responsible for allowing only a specific type of ions to pass. The selectivity filter is only a few angstroms wide hence the ions have to move through it in a single file fashion without their hydration shell [18].

A large number of ion-channels have been successfully crystallized over the last decade and x-ray crystallographic data have provided us with structural understanding of these protein complexes on the atomic level [19–22]. In parallel based on this data and by using molecular dynamics simulation different functional models for the mechanisms of ion selectivity and conduction have been developed [23–27], however experimental observation of these dynamics in real time and on atomic level has remained challenging.

Amongst the best studied ion-channels are potassium channels. Their family includes a wide range of channels with different conductivities and gating mechanism including the voltage gated potassium channels which are responsible for restoring the membrane potential during the course of action potentials in neurons [16]. While the gating mechanism can greatly vary across different types of potassium channels, the sequence of amino acids forming the selectivity filter is fairly conserved across all potassium channels. The structure of the selectivity filter has been best studied in the bacterial KcsA channel [19] on which the following discussions are focused.

During its open gate state an efflux of 10^8 ions per second can be experimentally observed [28] which is close to the diffusion limited rate. At the same time the selectivity filter is capable of selecting potassium over sodium with a ratio of at least $10^4 : 1$ [19]. Furthermore, it is known from the x-ray crystallographic data of the KcsA that its selectivity filter forms a pore with the diameter of ~ 0.3 nm and a length of ~ 1.2 nm. This implies that individual potassium ions cannot move through the selectivity filter with their 8 water molecule hydrated shell which must be shed before entering the selectivity filter. The transfer through the filter then proceeds in single file fashion where potassium and water molecules alternate. This makes the mentioned observations on transmission and discrimination rates even more remarkable. In a number of models of the selectivity filter this fact is accounted for by assuming that the ion transport is achieved via an interplay of ion - filter attraction and ion - ion repulsion while the selectivity is achieved through a mechanism which exploits the lower water shell dehydration energy for potassium than for sodium [23, 28, 29]. Certainly, the magnitude of the thermal fluctuations of the backbone atoms forming the selectivity filter is large relative to the small size difference between Na and K, raising fundamental questions about the mechanism that gives rise to ion selectivity. This suggests that the traditional explanation of ionic selectivity should be reexamined [18].

A closer look at the involved dimensions and energet-

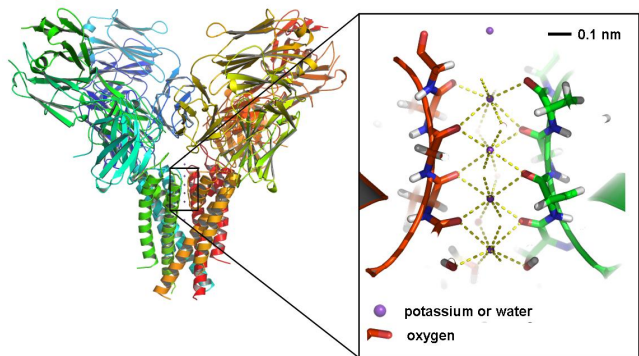


FIG. 1: Schematic illustration of the KcsA postassium channel after PDB 1K4C. KcsA protein complex with four transmembrane subunits (left) and the selectivity with four axial trapping sites formed by the carbonyl oxygen atoms in which a potassium ion or a water molecule can be trapped.

ics of the process reveals that the underlying mechanism for ion transmission and selectivity might be not entirely classical. Fig.1 shows the structure of the KcsA and the details of the selectivity filter. It is formed by four chains of amino acids each from one of the four protein complex subunits constituting the ion channel. Each chain is made of five amino acids from whom a carbonyl group oxygen atom is pointing toward the pore (Fig.1 inset). This configuration leads to a series of axial potential minima (i.e. binding sites) and maxima for the potassium ions. In each of these binding sites which are formed by four in plane oxygen atoms either a dehydrated potassium ion or a water molecule can be trapped (Fig.1 inset). Numerical calculations of free energy maps of the ion conduction shows two energetically nearly degenerate configuration paths for the ion transport which are separated by only ~ 2 kcal/mol [24]. The transport along each configuration path involves a coordinated dislocation of water -potassium chain. During these transitions different sequences of water and potassium occupy the four binding sites. This is also supported by the x-ray diffraction data which has revealed two equally represented populations corresponding to two different sequences of water and potassium in the filter which are referred to as 1,3 and 2,4 state [29]. In this arrangement the axial separation of the potential minima is ~ 0.24 nm and the height of the barrier fluctuates based on the presence or absence of an ion at a particular site and the thermal vibrations of the protein in the range of $\sim 1 - 5$ kcal/mol corresponding to $\sim 1.7 - 8k_B T$ [27]. This situation allows for at least two different but equivalent considerations through which quantum coherence could be involved in the ion transmission process.

First, based on the thermal energy of $E = k_B T/2 \approx 2 \times 10^{-21} J$ of the ions the de-Broglie wavelength $\lambda_{DB} = h/\sqrt{2mE}$ of the potassium matter wave can be estimated to be ~ 0.05 nm. Given that the periodicity of the axial modulation of the potential is ~ 0.25 nm it is within a factor of five of the potassium matter wavelength. In

this sense the transmission could involve a process which can be viewed as the diffraction of the potassium matter wave off a one dimensional axial "grating" formed by the modulations of the potential energy.

Alternatively the transmission could be seen to involve quantum tunneling through the potential barrier between individual neighboring binding sites. This can be seen by estimating the tunneling probability, $p_{tun} = e^{-\Delta\sqrt{2m(E_0-E)}/\hbar}$, with E the energy of a potassium ion, m , the mass of potassium, $E_0 - E$ the height and Δ the width of the tunneling barrier. Using the parameters of the selectivity filter [24, 27] this yields a tunneling probability of $\sim 7 \times 10^{-5}$ for a single "try". Multiplying this value with the trapping frequency of a bound ion in a harmonic potential of $\sim 10^{12} Hz$ yields an overall transmission approaching the observed rates of 10^8 ions per second. This estimate assumes a square well potential. However, a more accurate description would assume a quartic double well potential $V(x) = \alpha x^4 - 2\beta x^2$ whose parameters are chosen such that the potential barrier at $V(0)$ has a height $\Delta E = 0.04eV = 1.5kT$, and a separation of the minima of $\sim 0.24nm$. Furthermore, assuming that the degree of excitation inside a potential well will be compatible with the thermal energy, we can then compute the energy level splitting between levels that are split due to tunneling. This splitting gives the tunneling rate for a system in that energy level. Typical values range between $\sim 10^5 s^{-1}$ and $\sim 10^{10} s^{-1}$ for energy levels around the thermal energy. In these estimations we have assumed a static potential and have ignored any rotational vibration modes in the carbonyl groups. However, it has been theoretically shown [27, 30] that these could significantly lower the potential barriers, so that the tunneling probabilities given above would in this sense represent only a lower bound.

Based on these estimations we hypothesize that quantum coherence could be present in the selectivity filter and might be involved in explaining some of the functional features such as the high ion conduction rate and ion discrimination rate. However, given the strong interaction of the system with the environment these coherences may be short lived. A rough estimate suggests that the decoherence time will be on the order of $10^{-9} - 10^{-8} s$ and thus of the order of the expected tunneling rates [31]. In fact, we expect that the interplay between quantum coherent dynamics and decoherence from the environment might actually be necessary for explaining the dynamics of the selectivity filter. As demonstrated for the excitation transport through photosynthetic complexes the presence of dephasing noise [8, 9] may even enhance the efficiency of transport compared to the purely quantum coherent case.

A key feature of such coupled quantum systems that we will be exploiting here is that interference, constructive or destructive, in the underlying dynamics may lead to resonances in the transport efficiency. These resonances allow us to infer the presence of quantum coherence as they are absent in pure rate equation models. These res-

onances may be measured directly in the energy, particle or charge current that the systems allows – the measurement of correlations in time or coherence in relation to the driving field are not required.

This represents two distinct advantage. First the direct detection and verification of quantum coherence in biological systems has been so far based mainly on two (or higher) dimensional femtosecond spectroscopy techniques [32] in which quantum coherence manifests itself as a beating signal in the intensity of the cross peaks. In two-dimensional femtosecond spectroscopy three pulses and a strongly attenuated local oscillator are incident on the sample. The first pulse creates a coherence that evolves for a time period usually referred to as the evolution or coherence time, then the second pulse creates an excited-state population that evolves over a second time period called the waiting time or mixing period. Finally, the third pulse generates a coherence that accumulates phase in the opposite direction. Thereafter re-phasing occurs and a signal pulse is emitted in a direction determined by the phase matching condition. The coherence time and the detection time are scanned in a range of a few hundred picoseconds in the vibrational 2D spectroscopy and in the range of femtoseconds for studies in the visible range while the signal is measured through a heterodyne detection for each combination of the coherence and the detection time. In this way coupling strengths and energy transfer in molecules are probed. In the absence of coupling contributions from the excited-state absorption and emission cancel each other and as a result no off-diagonal peaks appear in the spectrum. In the presence of coupling the contributions from the excited state absorption and emission do not fully cancel and a so-called "cross peak" emerges in the spectrum. Intuitively speaking, the 2D spectroscopy can probe the "memory" of a system. As a result it can be used to examine how fast an initially coherent state decoheres with time.

Even though several laboratories are now mastering this method in the visible [1-3, 33] and in the IR regime [52-57] its implementation remains an experimental challenge. Besides the usual complexity involved in the design, operation and maintenance of a coherent ultrafast 2D spectroscopy system, it implies stringent requirements for stability and precision for the inter-pulse delay times.

Second, in some systems, such as in current-carrying polymers or in the selectivity filter the observation of resonances in transport rates may not only provide an alternative approach towards the verification of the existence of quantum coherence but also a means for direct demonstration of its importance for the system dynamics. Indeed, a further potentially significant implication of our work is that the presence of quantum coherence for example in the selectivity filter and the concomitant existence of sharp resonances in the transport may point towards a novel mechanism for the explanation of the high degree of selectivity. Indeed, relatively small changes in the sys-

tem parameters (mass, ion radius, interaction strengths of ions traversing the channel) may then lead to sharp changes in the conductance.

Quantum coherence & transport – The dynamics of ion conduction inside an ion channel is highly complex due to the manifold interactions between the ions and the multiple degrees of freedom of the channel. In the following quantum mechanical analysis of a transport process it is our aim to avoid this complexity while retaining some structural elements of the dynamics of an ion channel. This will allow us to show that in this simplified model quantum coherence can give rise to very significant effects in the conductance of the channel. In turn this suggests that a more realistic model may also exhibit similar features. This provides the motivation for considering possible experimental set-ups that would be able to verify or falsify the hypothesis of the presence of coherence in a real ion channel.

The theoretical and numerical discussion, first defines the basic dynamical equations governing the transport and discusses their relationship to real systems. Then we move on to demonstrate that coherently driven transport channels exhibit resonances in their conductance which, in turn, can be linked to the level of quantum coherence in the system. In fact, we will elucidate the mechanism behind these resonances and hence understand why they do not occur in systems exhibiting classical rate equation dynamics. Based on the insights that we gain from this analysis we then proceed to discuss in some detail the experimental feasibility of our predictions and discuss the concrete settings underlying our current experimental efforts in this direction.

The basic dynamical equations – In the present context we are focusing on quantum dynamical equations that are motivated by the example of the selectivity filter of ion channels. Nevertheless, their essential features should capture a wide variety of transport processes in bio-molecular systems. One of the underlying assumption is that to a good approximation the transport is particle number conserving, that is, it is described by a tight-binding type Hamiltonian that is mainly subject to dephasing-type noise. This is a reasonable model assumption for excitation transport in photosynthesis (excitation annihilation rates are short compared to the observed transport times) or the transport of ions through an ion channel (as ions rarely escape sideways through the channel walls). As we are principally motivated by ion channels we restrict attention to a linear chain of sites in which an excitation may be exchanged between nearest neighbors even though the ideas presented here are not limited to that setting. Note that an excitation at a particular site in the following Hamiltonian model does not need to represent the presence of a potassium ion at a certain position in space. Rather each site may also be thought of as specific potassium-water single file configurations that may arise during the transport. Each of these configurations will sit in an effective potential well and is separated from other configurations by a potential

barrier that it may traverse through quantum coherent tunneling or thermal activation [18]. The coherent part of the evolution is then described by the Hamiltonian

$$H/\hbar = \sum_{k=1}^N \omega_k(t) \sigma_k^+ \sigma_k^- + \sum_{k=1}^{N-1} c_k(t) (\sigma_k^+ \sigma_{k+1}^- + \sigma_k^- \sigma_{k+1}^+) \quad (1)$$

with hopping rates $c_k(t)$ and site energies $\hbar\omega_k(t)$ that may vary across sites and in time. Let us furthermore assume that the first and last site of the chain are connected to environments that insert or remove excitations from the system or, in other words, drive transitions between configurations. The first site may for example be linked to a source that supplies particles (electrons from a lead or potassium ions from the cytoplasm entering the ion channel thus driving the system to a different configuration) while the last site may then be linked to a similar environment but with lower voltage and/or lower concentration of particles. In general one may describe such processes by Lindblad [34] operators of the type

$$\mathcal{L}_{s/d}(\rho) = \Gamma_{s/d}(n_{s/d} + 1) [-\sigma_1^+ \sigma_1^- \rho - \rho \sigma_1^+ \sigma_1^- + 2\sigma_1^- \rho \sigma_1^+] + \Gamma_{s/d} n_{s/d} [-\sigma_1^- \sigma_1^+ \rho - \rho \sigma_1^- \sigma_1^+ + 2\sigma_1^+ \rho \sigma_1^-] \quad (2)$$

where s (d) stand for source (drain), Γ_s (Γ_d) for the coupling strength between the chain and the environments and where n_s (n_d) represent concentrations. Terms of the form $\sigma_1^+ \sigma_1^- \rho - \rho \sigma_1^+ \sigma_1^-$ are responsible for the evolution of the system when no excitation has entered or left the system, while the term $2\sigma_1^- \rho \sigma_1^+$ ($2\sigma_1^+ \rho \sigma_1^-$) describes the event when an excitation has left (entered) the system.

Dephasing noise also originates from an interaction with an environment, for example with the oscillatory degree of freedom of the carbonyl groups in the ions channel, but does not create or destroy excitations in the chain. Dephasing can be described by another Lindblad operator of the form

$$\mathcal{L}_{deph}(\rho) = \sum_k \gamma_k [-\{\sigma_k^+ \sigma_k^-, \rho\} + 2\sigma_k^+ \sigma_k^- \rho \sigma_k^+ \sigma_k^-] \quad (3)$$

with site dependent dephasing rates γ_k . It should be noted that this model ignores temporal and spatial correlations in the noise. While such correlated noise may lead to quantitative changes in the following considerations the basic principle of using the presence or absence of resonances in the conductivity to determine the presence of quantum coherence remains valid. Besides the coherent hopping between the sites there may also be thermally activated transitions between nearest neighbours. These would again be described by Lindblad operators of the form

$$\mathcal{L}_{th}(\rho) = \sum_{k=1}^{N-1} \Gamma_k^{th} \left[2\sigma_{k+1}^+ \sigma_k^- \rho \sigma_k^+ \sigma_{k+1}^- - \{\sigma_k^+ \sigma_{k+1}^- \sigma_{k+1}^+ \sigma_k^-, \rho\} \right] + \sum_{k=1}^{N-1} \Gamma_k^{th} \left[2\sigma_{k+1}^- \sigma_k^+ \rho \sigma_k^- \sigma_{k+1}^+ - \{\sigma_k^- \sigma_{k+1}^+ \sigma_{k+1}^- \sigma_k^+, \rho\} \right]. \quad (4)$$

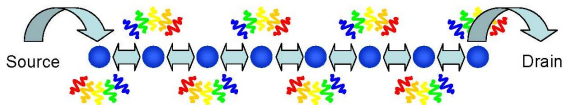


FIG. 2: A source drives excitations into the first site of a chain where nearest neighbors are coupled by a hopping interaction. The excitations leave the chain via the last site.

Hence the most general form of quantum dynamical equation that we will be considering here is of the form

$$\frac{d\rho}{dt} = -\frac{i}{\hbar}[H, \rho] + \mathcal{L}_s(\rho) + \mathcal{L}_d(\rho) + \mathcal{L}_{th}(\rho) + \mathcal{L}_{deph}(\rho). \quad (5)$$

To determine the conductivity of such a system we will consider $p_{sink}(t)$ which may be obtained directly by integrating the population of the last site multiplied with the net transfer from that site into the sink, that is

$$p_{sink}(t) = \int_0^T 2\Gamma_d \rho_{n,n}(t) dt.$$

As the current we will then define the asymptotic rate of growth of $p_{sink}(t)$ that is

$$I = \lim_{t \rightarrow \infty} \frac{dp_{sink}}{dt}(t). \quad (6)$$

Quantum coherence & conductivity – Now we would like to demonstrate that the conductivity of an externally driven channel exhibits resonances at which the conductivity is strongly suppressed. We will then show that the depth of these resonance reduces in the presence of dephasing noise and that it can be related to the amount of quantum coherence in the channel. Thus the depth of resonances may be taken as a measure for the presence of quantum coherence.

We consider a channel subject to a constant and a time dependent potential due to applied electric fields. Furthermore we assume, for simplicity and clarity of the argument, that the inter-site hopping rates are constant across the chain, i.e. $c_k = c$. In this case the coherent part of the dynamics is given by a Hamiltonian of the form

$$H/\hbar = \sum_{k=1}^N (\Omega_0 + \Omega_1 \cos \omega t) k \sigma_k^+ \sigma_k^- + \sum_{k=1}^{N-1} c (\sigma_k^+ \sigma_{k+1}^- + \sigma_k^- \sigma_{k+1}^+). \quad (7)$$

Here $\hbar\Omega_0$ is the energy difference between adjacent sites. In the ion channel this would be related to the energy difference between two close lying energy levels in adjacent potential wells. This difference may not exceed the level spacing in one of the potential wells which in turn tends to be below $10^{12} s^{-1}$. To achieve a transfer rate of the order of $10^8 s^{-1}$ through the channel, the effective hopping rate between sites should be of the same order

which in turn implies that $c^2/\Omega_0 \sim 10^8 s^{-1}$ if $c \ll \Omega_0$ as is the case for an ion channel.

In the limit of very long, ideally infinite chains, this Hamiltonian is known to exhibit the quantum coherent phenomenon of dynamic localization or dynamical suppression of tunneling, [35, 36]. The existence of this effect and its coherent character may be inferred from the following arguments. Consider a transformed picture in which the time-dependent on-site energies vanish at the expense of time dependent coupling strengths between the neighboring sites [36]. This is achieved by defining $A(t) = -\Omega_0 t - (\Omega_1/\omega) \sin(\omega t)$ to move to an interaction picture via the transformation $|\tilde{\psi}(t)\rangle = e^{-iA(t) \sum_k k \sigma_k^+ \sigma_k^-} |\psi(t)\rangle$. In this interaction picture the dynamics is governed by a Hamiltonian

$$H_I/\hbar = \sum_{k=1}^{N-1} c (e^{-iA(t)} \sigma_k^+ \sigma_{k+1}^- + e^{iA(t)} \sigma_k^- \sigma_{k+1}^+) \quad (8)$$

where now the coupling rates are time-dependent. For small c the hopping dynamics between neighbouring sites is slow compared to the time dependence $e^{\pm iA(t)}$ and averaging this Hamiltonian over the interval $[-\pi/\omega, \pi/\omega]$ we find that the effective Hamiltonian takes the form

$$H_I/\hbar = \sum_{k=1}^{N-1} c J_{\frac{\Omega_0}{\omega}} \left(\frac{\Omega_1}{\omega} \right) (\sigma_k^+ \sigma_{k+1}^- + \sigma_k^- \sigma_{k+1}^+). \quad (9)$$

Hence we expect that if $\Omega_0 = n\omega$ for some $n \in \mathbb{R}$ and E_1/ω coincides with a zero of the Bessel function J_n , then the evolution of a wave-packet becomes periodic in time and the spreading of the wave-packet and hence transport is suppressed. For an infinite chain this can be demonstrated rigorously [35, 36].

For a finite system that is in contact with a source and a sink, excitation transport will not vanish exactly. Firstly, within a time interval $[-\pi/\omega, \pi/\omega]$ the wavepacket will not be stationary but will oscillate changing its width. The localization length (the maximal extent over which the wavepacket may spread in that interval) may exceed the length of the channel and hence leave it into the sink. On the other hand the quantum coherence responsible for the localization will be perturbed by the incoherent processes that are taking place at source and sink. Nevertheless, it can still be expected that transport is suppressed significantly, even for short chains. Indeed, a numerical analysis confirms the presence of dynamic localization even for the dynamics of a short chain. Fig. 3 indeed demonstrates that with just 5 sites (similar results may be observed for shorter chains accompanied by higher oscillation frequencies ω), high contrast resonances in the conductivity can be observed and that these coincide very well with the zeros of the relevant Bessel-functions.

Note that the effective coupling rates in eq. (9) emerge through averaging over transition amplitudes and it hence becomes clear that the suppression of transport is a coherence effect. Another way to understand

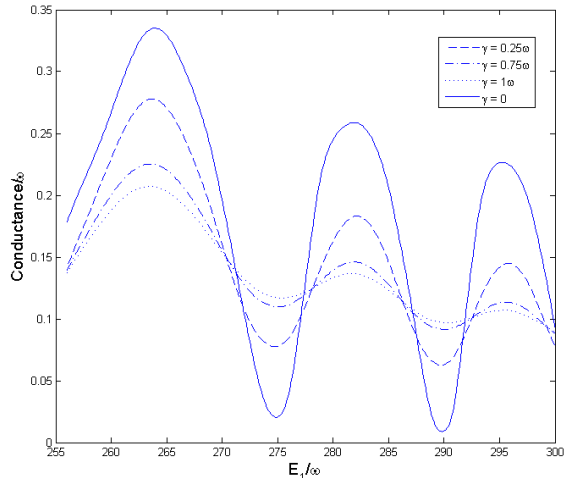


FIG. 3: Conductivity versus strength E_1 of the applied ac-potential for a chain with parameters $N = 5$, $\Omega_0 = 256 \cdot 10^8 s^{-1}$, $\Gamma_d = \Gamma_s = 10^8 s^{-1}$, $\omega = 2 \cdot 10^8 s^{-1}$, $n_T = 1$ and $c = 8 \cdot 10^8 s^{-1}$. For increasing dephasing rates $\gamma = 0, 5 \cdot 10^7 s^{-1}, 1.5 \cdot 10^8 s^{-1}$ and $2 \cdot 10^8 s^{-1}$ one observes a reduction in the depth of conduction resonances.

these results is from the observation that the ac-field will let the onsite energies oscillate so that periodically in time the neighboring sites become energetically close enough so that a coupling c that is insufficient to bridge an energy-gap of the order of E_0 will then induce transitions. In fact, this is the periodic analogue of the mechanism by which dephasing helps to overcome energy gaps [10]. However, in the periodic case, the wrong timing, can lead to coherent suppression of transport as well [40]. The physical origin of this trapping, and its quantum nature, may be understood by considering the extreme case of the Hamiltonian $H/\hbar = \sum_{k=1}^{N-1} \frac{c}{2} [1 + \text{sign}(\sin(\omega t + k\pi))] (\sigma_k^+ \sigma_{k+1}^- + \sigma_k^- \sigma_{k+1}^+)$ that is the couplings are switched on and off with a frequency ω alternatingly between neighboring pairs of sites. Within this model it is now easy to see why time-varying coupling rates may suppress transport in a quantum setting. For $\omega = c$ we observe that $\exp^{-iH_{eff}\pi/\Omega} |1\rangle = -|1\rangle$ and as a consequence excitations do not propagate at all. Hence, we expect that for certain frequencies transport will be suppressed [41].

All these arguments show that the dynamic suppression of transport relies on the existence quantum coherence, either through the destructive interference of transition amplitudes or the existence of full oscillations between sites. In purely classical rate equation models or strongly decohered quantum systems these effects will not exist. There is no destructive interference nor can the population between neighboring sites oscillate perfectly as it will rather approach an equilibrium value in which both sites will be populated. As a consequence we will not observe complete suppression of transport in a

classical rate equation models with time-modulated coupling rates between sites. In this sense dephasing may in fact assist the transport as it suppressed destructive interference at the resonance points.

The expected sensitivity of this phenomenon to the presence of decoherence can be seen in Fig. 3. Decreasing depth of the conductance resonances is associated with increasing levels of decoherence which in turn can be expected to be associated with decreasing levels of quantum coherence in the system. This is indeed a crucial observation as it allows us to turn the situation on its head and *use the depth of the contrast of the resonances as a tool to determine quantitatively the presence or absence of quantum coherence in the system* from measurement of its conductivity.

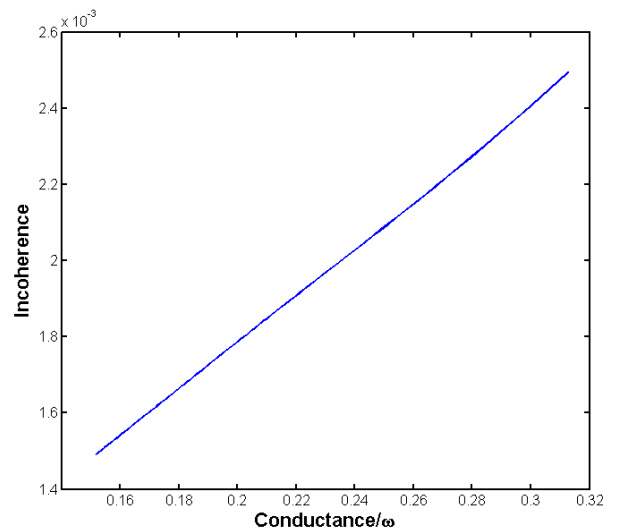


FIG. 4: Incoherence versus conductivity at the first resonance of fig. 3. The best fit to the data suggest that incoherence is proportional to conductivity.

There is no unique measure for the level of quantum coherence or incoherence in a state but the observed direct relationship hold true for a variety of measures. As a measure of incoherence, the quantity $\mathcal{C} = \sum_{k \neq l} |\rho_{k,k} \rho_{l,l} - \rho_{k,l} \rho_{l,k}|$ has the desirable properties that it vanishes for pure states, increases with decreasing size of the diagonal elements and is maximized for maximally mixed state. In addition \mathcal{C} is concave, that is, it increases under mixing of quantum states. For the first resonance in Fig. 3, comparing the depth of the conductivity resonance with the depth of the resonance in the quantum incoherence \mathcal{C} for different levels of dephasing noise, we find Fig. 4. This result is very well fitted by $\mathcal{C} \sim I$. It is this relationship that we would like to exploit for the detection of quantum coherence from the observation of currents in a modulated ion channel.

Theory Discussion & Speculation – The results above demonstrate that systems that are governed by coherent quantum dynamics will, for certain choices of parameters,

exhibit resonances in their transport efficiency, i.e. conductivity. As these resonances are absent in purely classical rate equation models or in quantum systems subject to very strong decoherence, the observation of currents, for example in periodically driven ion channels, provides an interesting alternative for the observation and verification of the presence of quantum coherence.

These resonances, caused by quantum coherence, are relatively sharp features in parameter space. As a consequence, in the presence of quantum coherence, the dynamics is much more sensitive to small variations of system parameters such as ion mass, ion radius etc. In purely classical models the rather small differences in diameter between potassium and sodium ions are not expected to result in significant changes in the ion conduction. In addition to the effects on the conduction rate presented above one may speculate, whether the enhanced sensitivity of the quantum dynamics may contribute to the selectivity of the filter of the ion channel.

Needless to say, the dynamics of ion conduction in ion channels is in fact a many-body phenomenon in which many degrees of freedom interact. Recent numerical simulations of the ion-transfer [27] suggest for example that the multi water-potassium chain does not move as one unit but rather in discrete units of individual water-potassium translocations, in which the translocation of a potassium ion to the next site is followed by the water molecule in picosecond time scale. Given the short time scale for this substructure of the transport process it provides an additional mechanism through which quantum coherence may appear.

Of course such dynamics is considerably more complex than the model Hamiltonians described here more rigorous conclusions in that direction need to await more detailed simulations and experimental investigations [30].

Experimental realization – As mentioned earlier, it is an advantage of the model presented above that it provides experimentally testable predictions for the existence of coherent excitations in the selectivity filter through the observation of driven quantum resonances. This is experimentally particularly attractive as the presence of coherence can be inferred via the measurement of bulk signals, eliminating some of the challenges associated with alternative and more direct methods such as 2D femtosecond spectroscopy. As shown in Fig.3 in the presence of coherence at certain frequencies of an external driving field, the ion conduction through the selectivity filter can be highly impaired. This would be in sharp contrast to what should be observed when dephasing is destroying all coherence and the conduction of ions is governed by pure rate processes making it essentially independent of the amplitude of the alternating external driving force.

There might be several ways for testing this prediction experimentally. In the following we would like to discuss one of these in some detail to demonstrate the in-principle feasibility of such measurements. One could for example be using state of the art electrophysiology

methods with some modifications for adapting them to the particular conditions that are required for resonances in ion channels to be observed. Electrophysiology techniques such as patch clamping [42] have found applications in a large number of biophysical studies for recording single ion channel currents. During the open gating period of a few *ms* these currents can be observed experimentally in different patch clamp techniques such as the cell attached mode and the excised patch configuration [42]. In these methods a glass pipette with an inner diameter of $1\mu\text{m}$ is filled with an electrolyte and is used to make a high resistance ($> 10^9\Omega$) seal with the cell membrane. Generally, only a few ion channels can be present on a membrane patch of that size. Because of the high resistance of the seal any exchange of ions between the electrolyte in the pipette and the bath (or the cell cytoplasm) passes through the ion channels. Voltage-gated channels have single-channel conductances typically range from $10 - 100\text{pS}$. They last over the few *ms* open period of the gate are amplified by a current to voltage converter and recorded.

Here we should mention that the fact that multiple ion channels could be present on a membrane patch of the size of pipette tip by no means affects the experimental signature of quantum coherence in a negative fashion. As discussed above the manifestation of quantum coherence in the selectivity filter would be observable as a change in the "bulk" ionic current through the channel as a function of the externally applied AC driving force. In that sense as long as the driving force is constant over the number of channels, it actually represents an advantage to have more channels within the patched area, as it would help in increasing the signal to noise ratio.

But in order to be able to apply electrophysiology methods to experimentally drive the resonances in the selectivity filter and record the transmitted ion rate several conditions have to be met. These will be discussed in some detail in the remainder of this work.

In contrast to many single ion channel studies in which investigators are interested in the gating dynamics of the channel, our recordings have to be made during the open state of the channel. This requires the reliable preparation of the channel in its open gate state. Since the structure of the selectivity filter is highly conserved across the potassium channel family the experiments can also be done in Kv voltage gated potassium channels [43]. For this category of potassium channels a number of pharmacological agents are available which can be used to initiate the open state of the channel. Alternatively, a class of potassium channels, the calcium activated potassium channels [43–45] can be used in which the open conformation can be triggered by adding calcium to the bath. Finally, it is also possible to introduce site mutations in the voltage sensor region or use enzymes which impair the function of the voltage sensor and lead to permanently open channels [46].

Next, it is necessary to establish an ionic current across the channel in the absence of the AC driving force.

Again, while this could be done through a current injection via the patch clamp amplifier, it would be more convenient and also reassemble the natural conditions by establishing a potassium concentration gradient across the ion channel. The role of the potassium channel during the action potential is to restore the membrane potential from $\sim +30mV$ after the fast opening of the sodium channels back to the resting membrane potential of $\sim -70mV$. During this period potassium flows out of the cell along its concentration gradient ($90mM$ intracellular vs. $3mM$ extracellular). Given the equilibrium potential [16] of potassium of $-85mV$ at this concentration difference this represent a driving force of $115mV$. For our experimental considerations it would not be necessary to hold the membrane potential at $+30mV$. Once the potassium concentration difference ($90mM$ intracellular vs. $3mM$ extracellular) is generated by adding more potassium to the patch pipette than to the bath, even at $0mV$ membrane potential, a driving force of $85mV$ for the ions would be available. If we assume an excised patch configuration in which a the current through a few channels on a dissociate patch of membrane sealed to the pipette is measured, this driving force will establish a constant current of a few pA . This constant driving force and the associated ionic current represent E_0 in equation (7).

In order to observe the predicted quantum resonances via the ionic currents through the channel an alternating driving potential, $E_1 \cos \omega t$ with the frequency ω has to be applied across the channel. This frequency ω should be chosen to exceed the effective hopping rate in our theoretical model which in turn is expected to be of the order of the ion channel transmission rate, i.e. around $10^8 s^{-1}$. As argued before, for an energy difference $\hbar\Omega_0$ between adjacent potential wells, the resonances will be found at the zeros of the Bessel function $J_{\Omega_0/\omega}$. We can expect $\Omega_0 \gg \omega$ and hence the first zero of the Bessel function $J_{\Omega_0/\omega}$ is, in leading order, located at $\Omega_1/\omega \cong \Omega_0/\omega$ [47]. The required ac-field could be applied across the channel by using an external function generator synchronized with the amplifier. Alternatively an RF field at the same frequency with its polarization aligned along the axis of the ionic propagation might be used as an alternating driving force.

However, because of the high frequency of the AC field the membrane capacitance and the stray capacitance of the pipette glass will lead to additional capacitive currents significantly higher than the membrane current. Moreover, the time constant τ for establishing a potential difference across the membrane is given by $\tau = C_m R_p$, with C_m the membrane capacitance and R_p the pipette resistance. Therefore it would be desirable to minimize the area of the membrane patch across which the AC field is applied. This limitation excludes any whole cell recordings and limits our considerations to the excited patch configuration for which the membrane capacitance is minimized as it will be determined by the surface area of the pipette tip. (see Fig 5). The excised patch config-

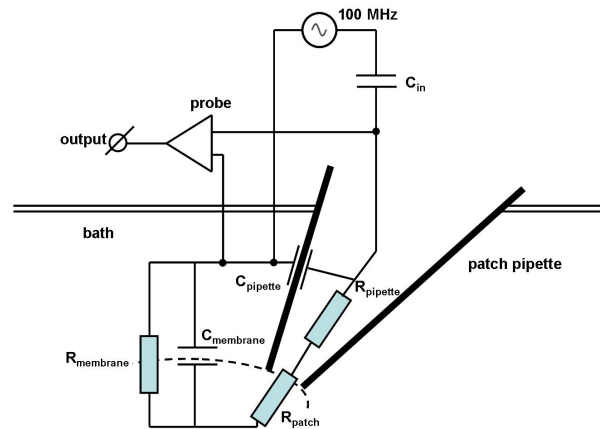


FIG. 5: Equivalent circuit for the excised patch configuration and external driving force to induce quantum resonances.

uration is also advantageous as it allows the study of the ion channels in isolation and provides better control for the application agents on both sides of the channel.

Assuming an inner diameter of $1\mu m$ and a typical membrane capacitance of $C_m \sim 1\mu F/cm^2$ this results in a membrane capacitance of $C_m \sim 8 \times 10^{-15} F$. As we would like to apply an AC field at $100MHz$ the time constant τ should be at least $5ns$. Based on the membrane capacitance of $C_m \sim 8 \times 10^{-15} F$ estimated above, it means that the pipette resistance R_p should not be larger than $0.6M\Omega$. Typical pipette resistances are in the range of tens of $M\Omega$, but it should be possible to reduce these values by appropriate shaping of the pipette tip.

Further, the mentioned capacitive currents required some careful considerations. As shown in Fig 5 the membrane capacitance C_m and the pipette capacitance C_p are both contributing to the induced capacitive currents by the fast alternating AC field. While the membrane capacitance can be minimized by using the excised patch configuration, minimizing the pipette capacitance requires using special type of glasses [48], minimizing the level of the electrolyte in the pipette and coating the pipette with insulating raisins which would thicken the external pipette walls and reduce the stray pipette capacitance. This can be done by coating the pipette with a layer of Sylgard, an inert, hydrophobic, translucent elastomer raisin which is cured rapidly by heat [49]. These measures could reduce the pipette capacitance to $C_p \sim 10^{-13} F$. However, this would be still about an order of magnitude larger than C_m and therefore the major contributor to the capacitive current.

As discussed above the applied AC field has to induce a membrane potential change of $315mV$ in $10ns$. With C_p as the dominating factor this means that the AC field would lead to a capacitive current of $3\mu A$ which is six orders of magnitude higher than the pA ionic currents through the channel. It could be somewhat challenging

to separate these two components, however the difference in the timing of these currents could provide the means to separate them. The above choice for the time constant τ is such that the peaks of the capacitive currents are separated by the period of the AC field. Therefore a lock in detection technique can be used to reject the capacitive currents and isolate the ionic current. Moreover for a fixed frequency (e.g. 100MHz) it is possible to design additional electronic circuits which introduce negative capacitance to compensate the capacitive currents. Finally a number spectral analysis technique can be applied to isolate the ionic current from the capacitive currents. Another approach which could eliminate the pipette capacitance altogether is to use chambers with suspended planar phospholipids bilayers in which the ion channels have been reconstituted [50]. In this technique the two macroscopic chambers filled with electrolytes are separated by an artificial lipid layer in which the ion channels have been reconstituted. Ions can move along their concentration gradient only through the ion channels and are recorded and amplified with a same amplifier system as discussed above. The AC field can be applied between the two chambers, while the current through the membrane is monitored. Since in this approach the pipette is

eliminated the only source for capacitive currents is the lipid membrane. However in such a setup the membrane area is typically larger than the in the patch pipette so that it might lead only to a moderate reduction of the capacitive currents.

Finally, the recent development of NV-centers point to an alternative method for recording pico-Ampere currents in biological systems with high spatial and temporal control [51].

On the positive side the fact that the flux rate of ions at a given concentration is fairly constant and the fact that the width of the expected quantum resonances in Fig. 3 is not very sharp, is expected to help finding these resonance experimentally.

Overall the above assessments show that currently available techniques from single channel biophysics studies with moderate modification can be adopted and used for experimental investigations of quantum resonances in the selectivity filter of potassium channels.

Acknowledgements – This work was supported by an Alexander von Humboldt-Professorship and by the Howard Hughes Medical Institute. Correspondence should be addressed to vaziria@janelia.hhmi.org or to martin.plenio@uni-ulm.de.

-
- [1] G.S. Engel, T.R. Calhoun, E.L. Read, T.-K. Ahn, T. Mancal, Y.-C. Cheng, R. E. Blankenship & G.R. Fleming, *Nature* **446**, 782 (2007).
- [2] I.P. Mercer, Y.C. El-Taha, N. Kajumba, J.P. Marangos, J.W.G. Tisch, M. Gabrielsen, R.J. Cogdell, E. Springate, and E. Turcu, *Phys. Rev. Lett.* **102**, 057402 (2009).
- [3] G. Panitchayangkoon, D. Hayes, K.A. Fransted, J.R. Caram, E. Harel, J. Wen, R.E. Blankenship, G.S. Engel, E-print arXiv:1001.5108
- [4] R. W. Schoenlein et al., *Science* **254**, 412, (1991)
- [5] Q. Wang, *Science* **266**, 422, (1994)
- [6] S. Hecht, S. Schlaer, and M.H. Pirenne, *Energy, Quanta and Vision, Journal of the Optical Society of America*, **34** 38, 196 (1942)
- [7] D. A. Baylor, T. D. Lamb, and K. W. Yau, *Journal of Physiology*, **288**, 613 (1979)
- [8] M. Mohseni, P. Rebentrost, S. Lloyd, and A. Aspuru-Guzik, *J. Chem. Phys.* **129**, 174106 (2008).
- [9] M.B. Plenio and S.F. Huelga, *New J. Phys.* **10**, 113019 (2008).
- [10] F. Caruso, A. Chin, A. Datta, S.F. Huelga and M.B. Plenio, *J. Chem. Phys.* **131**, 105106 (2009).
- [11] A.W. Chin, A. Datta, F. Caruso, S.F. Huelga, M.B. Plenio, E-print arXiv:0910.4153 [quant-ph]
- [12] J.S. Cao and R.J. Silbey, *J. Phys. Chem. A* **113**, 13825 (2009)
- [13] A. Olaya-Castro, C. Fan Lee, F. Fassioli Olsen, N.F. Johnson, *Phys. Rev. B* **78**, 085155 (2008).
- [14] S. Hoyer, M. Sarovar and B. Whaley, E-print arXiv:0910.1847.
- [15] F. Caruso, A.W. Chin, A. Datta, S.F. Huelga, M.B. Plenio, E-print arXiv:0912.0122; F. Fassioli and A. Olaya-Castro, E-print arXiv:1003.3610.
- [16] B. Hille, 3rd edn Sinauer, Sunderland, Massachusetts (2001).
- [17] D. Triggler, ed., John Wiley & Sons (2006).
- [18] B. Roux and K. Schulten, *Structure* **12**, 1343 (2004).
- [19] D. A. Doyle et al., *Science*, **280**, 69 (1998).
- [20] R. Dutzler et al., *Nature*, **415**, 287 (2002).
- [21] O. Sokolova, L. Kolmakova-Partensky, and N. Grigorieff, *Structure*, **9**, 215 (2001).
- [22] M. C. Wang et al., *Journal of Biological Chemistry*, **279**, 7159 (2004)
- [23] S. Y. Noskov, S. Berneche, and B. Roux, *Nature*, **431**, 830 (2004).
- [24] S. Berneche, and B. Roux, *Nature* **414**, 73 (2001).
- [25] A. V. Dmitriev et al., *Biofizika* **51**, 698 (2006).
- [26] S. Garafoli, and P. C. Jordan, *Biophysical Journal* **84**, 2814 (2003).
- [27] J. F. Gwan, and A. Baumgaertner, *Journal of Chemical Physics* **127** (2007).
- [28] E. Gouaux, and R. MacKinnon, *Science* **310**, 1461 (2005).
- [29] J. H. Morais-Cabral, Y. F. Zhou, and R. MacKinnon, *Nature* **414**, 37 (2001)
- [30] Work in progress
- [31] To estimate the expected decoherence time we assume that the dominant form of noise stems from the stretch mode of the carbonyl groups in the ion channel. Their resonance frequency is approximately $\omega_{CO} \sim 3.2 \cdot 10^{14} \text{ s}^{-1}$ corresponding to a wave number of around 1700 cm^{-1} . Hence, at room temperature, this oscillation is essentially in the ground state. This zero point motion gives rise to a mean square deviation of the position of the oxygen atoms of the order of 0.02 \AA . The oxygen atoms in the carbonyl group carry an effective negative charge and hence

their motion will affect the potential that charges such as potassium ions experience in the ion channel. The fluctuating potential leads to fluctuating energy differences between two potential wells which in turn are responsible for dephasing of superposition states between two wells. The potassium ions in their potential wells have a frequency of around $\omega_K \sim 3 \cdot 10^{12} s^{-1}$. Numerically one can now determine that the zero-point motion of the carbonyl groups will affect the energy difference between two wells by around $\hbar\omega_K/10$ for a typical displacement. This leads to a coupling of the oscillations of the carbonyl groups to that of the potassium ions. Now we treat this as a simple two-mode quantum system, one mode referring to the oscillation of the carbonyl group and the other to the energy difference between two potential wells. The Hamiltonian is given by $H = \hbar\omega_{CO}a^\dagger a + \hbar\omega_K(X_{CO})b^\dagger b \cong \hbar\omega_{CO}a^\dagger a + 0.1\hbar\omega_K(a + a^\dagger)b^\dagger b + \hbar\omega_K b^\dagger b$. Here $\hbar\omega_K$ denotes the energy difference between two potential wells which is in turn a function of the position of the oxygen atom in the carbonyl group. Now initialising the system in the state $|0\rangle_a(|0\rangle + |1\rangle)_b$ corresponding to a superposition of an ion in the left or right potential well we find that the time in which the fidelity with the initial state has dropped to $1/e$ is around $3000\omega_K^{-1}$ suggesting that the decoherence time is of the order of $t_{dec} \sim 3000\omega_K^{-1} \sim 3 \cdot 10^{-9} s$. This is of the order of the tunneling time. It should be noted that there are a variety of unknowns that may affect the decoherence time. On the one hand we have ignored the oscillation of the carbon, nitrogen and hydrogen in the ion channel which may lead to a slightly higher decoherence rate. We have neglected oscillations along the channel axis as these have a much smaller effect on the potential and hence couple more weakly to the potassium ions. On the other hand the present estimate assumes a first order effect of the oscillation of the carbonyl group on the potential in the ion channel. If the system was making oscillations around equilibrium the potential change would be a second order effect and hence smaller. Hence the quoted figure provides a ball park figure but may vary somewhat. Furthermore, it should be noted that these oscillations do not only lead to a dephasing between two potential wells but also affects the height of the potential barrier. In fact, the line width $\Delta\omega$ due to the oscillations and the variations in the height of the potential barrier are approximately proportional. As the tunneling rate is strongly non-linear with the potential barrier height it can be expected that these oscillations can actually be beneficial.

- [32] R. M. Hochstrasser, Proceedings of the National Academy of Sciences of the United States of America **104**, 14190 (2007).
- [33] E. Collini and G.D. Scholes, Science **323**, 369 (2009).
- [34] D. Walls and G. Milburn, *Quantum Optics*, Springer Verlag, Berlin.
- [35] D.H. Dunlap and V.M. Krenke, Phys. Rev. B **34**, 3625 (1986).
- [36] M. Holthaus and D.W. Hone, Phil. Mag. **B 74**, 105-137 (1996).
- [37] K. Eckert, O. Romero-Isart and A. Sanpera, New. J. Phys. **9**, 155 (2007).
- [38] F. L. Semião, K. Furuya, G. J. Milburn, E-print arXiv:0909.1846.
- [39] A. Asadian, M. Tiersch, G.G. Guerreschi, J. Cai, S. Popescu, H.J. Briegel, E-print arXiv:1002.0346.
- [40] Consider $H/\hbar = \sum_{k=1}^{N-1} \frac{c}{2} [1 + a \cdot \sin(\omega t + k\pi)] (\sigma_k^+ \sigma_{k+1}^- + \sigma_k^- \sigma_{k+1}^+)$ where $0 \leq a \leq 1$ and the coupling rates between neighbouring pairs oscillate with opposite phase. The resulting Hamiltonian can be solved exactly in the limit of $N \rightarrow \infty$ as it is invariant by a shift of two sites and exhibits dynamic localization. Indeed, an excitation initially localized in site 1 will not propagate through the system completely but a portion, depending on the size a , is trapped depending.
- [41] Note that for the case $\omega = 2c$ we observe a certain enhancement of the transport because $\exp^{-iH_{eff}\pi/\omega} |1\rangle = i|2\rangle$ so that at the end of the interval $[0, \pi/\omega]$ the population has been transferred perfectly to site 2. In the next time interval sites 2 and 3 are now coupled with the same strength and as a consequence the population is transferred perfectly to site 3 and so forth. Hence the population is transported without any spreading and at the maximum speed given the coupling rate c through the chain.
- [42] B. Sakmann, and E. Neher, Springer-Verlag New York, LLC (1995).
- [43] G. Yellen, Nature **419**, 35 (2002).
- [44] Y. X. Jiang et al., Nature **417**, 515 (2002).
- [45] M. A. Schumacher et al., Nature **410**, 1120 (2001).
- [46] T. Hoshi, W. N. Zagotta, and R. W. Aldrich, Science **250**, 533 (1990).
- [47] H. Jeffreys and B. Swirles Jeffreys, *Methods in Mathematical Physics*, Cambridge University Press.
- [48] D. Odgen, The Company of Biologists Ltd. (1994).
- [49] J. L. Rae, and R. A. Levis, Methods in Enzymology **207**, 66 (1992).
- [50] C. Miller, Plenum Press (New York)
- [51] L.T. Hall, C.D. Hill, J.H. Cole, B. Stdler, F. Caruso, P. Mulvaney, J. Wrachtrup, L.C.L. Hollenberg, E-print arXiv:0911.4539
- [52] P. Hamm, M. Lim, R.M. Hochstrasser, J. Phys. Chem. B **102**, 6123 (1998).
- [53] M. Khalil and A. Tokmakoff, Chem. Phys. **266**, 213 (2000).
- [54] N. Demirdoven, M. Khalil, A. Tokmakoff, Phys. Rev. Lett. **89**(2002).
- [55] I.J. Finkelstein, J.R. Zheng, H. Ishikawa, S. Kim, K. Kwak, M.D. Fayer, Phys. Chem. Chem. Phys. **9**, 1533 (2007).
- [56] A. Tokmakoff, Science **317**, 5834 (2007).
- [57] J. Brendenbeck, J. Helbing, C. Kolano, P. Hamm, Chem. Phys. Chem. Phys. **8**, 1747 (2007).